



Silica Supported Copper-Nickel Oxide Catalyst for Photodegradation of Methylene Blue

A.K. PROD JOSANTOSO^{*ID}, S. KAMILIA, M.P. UTOMO^{ID} and K.S. BUDIASHIH^{ID}

Department of Chemistry, Yogyakarta State University, Yogyakarta, DIY 55281, Indonesia

*Corresponding author: E-mail: prodjosantoso@uny.ac.id

Received: 22 June 2019;

Accepted: 13 August 2019;

Published online: 16 November 2019;

AJC-19637

Organic wastes are often harmful for organisms living in water. The compounds may be toxic and/or carcinogenic. Many methods have been applied to minimize the organic wastes in water, one of which is through photodegradation process using catalysts. This report is about the use of $(\text{Cu-Ni})\text{O}_x/\text{SiO}_2$ catalyst for photodegradation of methylene blue under sunlight exposure. A series of methods including XRD, SEM-EDX and UV-visible spectroscopy has been used in the study. The catalyst adsorption test was carried out in the dark environment, whilst the catalyst activity test in photodegradation of methylene blue was performed under sunlight. The measurements on $(\text{Cu-Ni})\text{O}_x/\text{SiO}_2$ catalyst clearly indicate the presence of tridymite silica (SiO_2) with the particle size around 9 nm. The silica band gap energy decreases with the adsorption of copper and nickel on the surface of silica. The adsorption follows the Langmuir adsorption isotherm. The $(\text{Cu-Ni})\text{O}_x/\text{SiO}_2$ is significantly catalyzed the degradation of methylene blue in water.

Keywords: Copper oxide, Nickel oxide, Photocatalysts, Methylene blue.

INTRODUCTION

The current development of textile industry has increased the use of dyes, that can pollute the environment. The waste produced from the textile industry is generally non-biodegradable organic compounds, which can cause aquatic pollution [1]. Moreover, dyes in the water bodies can also affect the diversity of waters, because dyes block the penetration of light entering the water [2].

Methylene blue is one of the thiazine dyes that is often used by the textile industry, because of the price and the availability. Methylene blue is a basic dyestuff that is important in the process of fabrics colouring. The methylene blue can cause several negative effects, such as irritation of the digestive tract, cyanosis and irritation to the skin [3]. Because of its dangerous nature, a good method is needed to remove dyes from industrial waste water before being released into the aquatic environment.

In general, many methods of handling textile waste have been developed including the adsorption method and membrane filtration process. The disadvantage of the membrane filtration method is that the short service time and regular membrane replacement can add to the costs. Above all the

processes for removing colour, the adsorption method is a widely applied process [4]. However, this method turned out to be less effective because the textile dyes adsorbed accumulated in the adsorbent which would cause new problems [5].

In addition, the degradation method uses microbial assistance and is a bioremediation system that is widely applied to industrial waste treatment systems [6]. However, processing with this method requires a large area. Moreover, complex structure dyes that are removed will be difficult to degrade. Chemical methods such as coagulation or flocculation which can remove colour were introduced to overcome some problems relating with organic waste treatment [7]. However, processing using this method is likely to cause a new disposal problem because it may produce a considerable amount of chemical sludge which requires relatively high costs. In addition, the mud produced will also create new problems [8].

In general, these methods are quite effective but require high operational costs. Relatively cheaper and more effective methods are deserved. Alternatively, photodegradation method is used. The photodegradation method is effective in decomposing dyes with the help of photocatalysts and light into harmless compounds such as H_2O and CO_2 without causing new waste [9]. The advantages of using photocatalysts include the ability

of the catalysts to mineralize organic pollutants including textile wastes which contain azo compounds, non-toxic, high durability, low cost, fast and effective processes, reuseability and environmental friendly [10].

The photocatalyst used in photodegradation process accelerates the decomposition of the dyes simultaneously or and continuously. The photocatalysts used usually are in the form of semiconductors. Photocatalyst oxide semiconductor materials that are often used are SiO_2 , TiO_2 and ZnO [11-13]. Silica is easily found in everyday life. The SiO_2 can also be obtained from organic or inorganic materials. The SiO_2 is applied in electronic devices, ceramics, cement adsorbents and is often used as a catalyst. In addition, SiO_2 can be used as a support that serves to increase catalyst efficiency.

Some researchers [14-16] improved photocatalytic activities by modifying the SiO_2 . The addition of metals in SiO_2 material is able to increase the spectral response to the visible area resulting in band gap shiftings [17].

The copper oxide is a p-type semiconductor with E_g between 1.2-1.9 eV [18] and suitable for photodegradation under visible light. In other hand, nickel oxide has a high catalytic activity [19]. The high surface area of metal oxide catalysts can be obtained from the calcination of the metal salts at high temperatures. Similarly, the supported metal oxide catalysts can be prepared by calcinating the supported metal salts. The supported metal salts can be prepared using impregnation method, which is relatively inexpensive, easy and effective [20]. The use of $(\text{Cu-Ni})\text{O}_x/\text{SiO}_2$ catalyst, which is prepared using impregnation method, for the photodegradation of the methylene blue under the sunlight exposure is reported.

EXPERIMENTAL

Impregnation method has been used to prepare the catalysts. The $(\text{Cu-Ni})\text{O}_x/\text{SiO}_2$ was made by mixing a proportional amount of $\text{Cu}(\text{NO}_3)_2 \cdot 3\text{H}_2\text{O}$ (Merck, 99-104 %) and $\text{Ni}(\text{NO}_3)_2 \cdot 6\text{H}_2\text{O}$ (Merck, 99.99 %), with 1.994 g of SiO_2 (E merck), where the mole percentages of Cu:Ni to Si is 0.3:0 %; 0.2:0.1 % and 0.15:0.15 %, followed by addition of distilled water to a total volume of 30 mL, stirring and evaporating to get an almost dry mixture. To the dry mixture 96 % ethanol solution was added and stirred and followed the addition of methanol and filtered. The isolated residue was air dried for 24 h. The dry residue was calcined at 800 °C for 4 h. Procedures were repeated using variations in the concentration of $(\text{Cu-Ni})\text{O}_x/\text{SiO}_2$ (0.3:0 %; 0.2:0.1 % and 0.15:0.15 %).

The adsorption of methylene blue on the $(\text{Cu-Ni})\text{O}_x/\text{SiO}_2$ was observed at the dark environment. The 0.1 g of $(\text{Cu-Ni})\text{O}_x/\text{SiO}_2$ was mixed with 50 mL of 10 ppm methylene blue solution in a 100 mL Erlenmeyer flask. The mixture was placed on top of the shaker in a dark compartment. The extract absorbance was measured at 0, 5, 10, 15, 20, 25, 35, 65, 95 and 125 min using spectronic working on a wavelength of 663 nm. The same procedure was undertaken under sunlight.

The powder of $(\text{Cu-Ni})\text{O}_x/\text{SiO}_2$ was studied by using XRD, SEM-EDX and UV-visible DRS. The XRD diffractograms of $(\text{Cu-Ni})\text{O}_x/\text{SiO}_2$ were collected by using X-ray diffraction Rigaku Multiflex, with the $\text{Cu-K}\alpha$ radiation, in the 2θ range from 5°-80°. The UV-visible spectrum of $(\text{Cu-Ni})\text{O}_x/\text{SiO}_2$

was recorded as a function of wavelength using the UV-visible 1700 Pharmaspec spectrophotometer specular reflectance. The samples of $(\text{Cu-Ni})\text{O}_x/\text{SiO}_2$ were put into cuvettes and measured using a UV-visible spectrophotometer in a wavelength range of 200-800 nm. Surface morphology analysis and composition of $(\text{Cu-Ni})\text{O}_x/\text{SiO}_2$ were qualitatively analyzed using scanning electron microscopy-electron dispersive X-ray analyzer JEOL JED-2300 operating in 15 kV and 5000x magnification.

RESULTS AND DISCUSSION

The grayish white $(\text{Cu-Ni})\text{O}_x/\text{SiO}_2$ catalysts have been prepared. The XRD diffractograms of $(\text{Cu-Ni})\text{O}_x/\text{SiO}_2$ can be seen in Fig. 1. A wide and weak peak at $2\theta = 21.6^\circ$ indicating tridimite SiO_2 (PDF data No. 39-1425) is observed. This is also confirmed by Srisittipokakun *et al.* [21] who prepared CuO/SiO_2 using bioorganic SiO_2 . The catalysts particle size determined using Scherrer equation [22] is 9.09 nm. Unfortunately, the XRD diffractograms unable to trace the presence of Cu or Ni species supported on the silica surface.

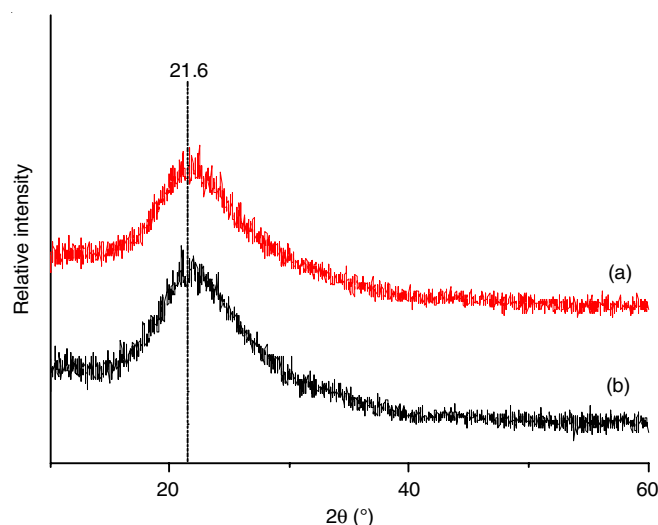


Fig. 1. XRD diffractogram of $(\text{Cu-Ni})\text{O}_x/\text{SiO}_2$ where (a) Cu:Ni = 0.2:0.1 and (b) Cu:Ni = 0.15:0.15

The $(\text{Cu-Ni})\text{O}_x/\text{SiO}_2$ catalyst morphology is dominated by irregular form particles having a rough surface and a range particle size of 1 to 15 μm (Fig. 2). The EDA method informs the presence of the elements qualitatively, but not quantitatively for the Cu and Ni metals (Fig. 3). This is probably caused by the too small number of those metal species on the support.

UV-visible spectrometry measurements were carried out for $(\text{Cu-Ni})\text{O}_x/\text{SiO}_2$ samples at wavelength range of 200-800 nm. The UV-visible spectra of the catalysts indicate that each sample experiences energy absorption at a certain wavelength (Fig. 4). The UV-visible absorbance peak of $(\text{Cu-Ni})\text{O}_x/\text{SiO}_2$ where Cu:Ni = 0.3:0 shifts towards the right, that is to the visible light region. This is promising since the sun light facilitates more visible than UV light. When compared to SiO_2 having large band gap energy and working only under UV light, the SiO_2 supported CuO_x is expected to broaden the working of the irradiation area of SiO_2 and reduce the band gap energy, so that $(\text{Cu-Ni})\text{O}_x/\text{SiO}_2$ where Cu:Ni = 0.3:0 may work effectively under visible light.

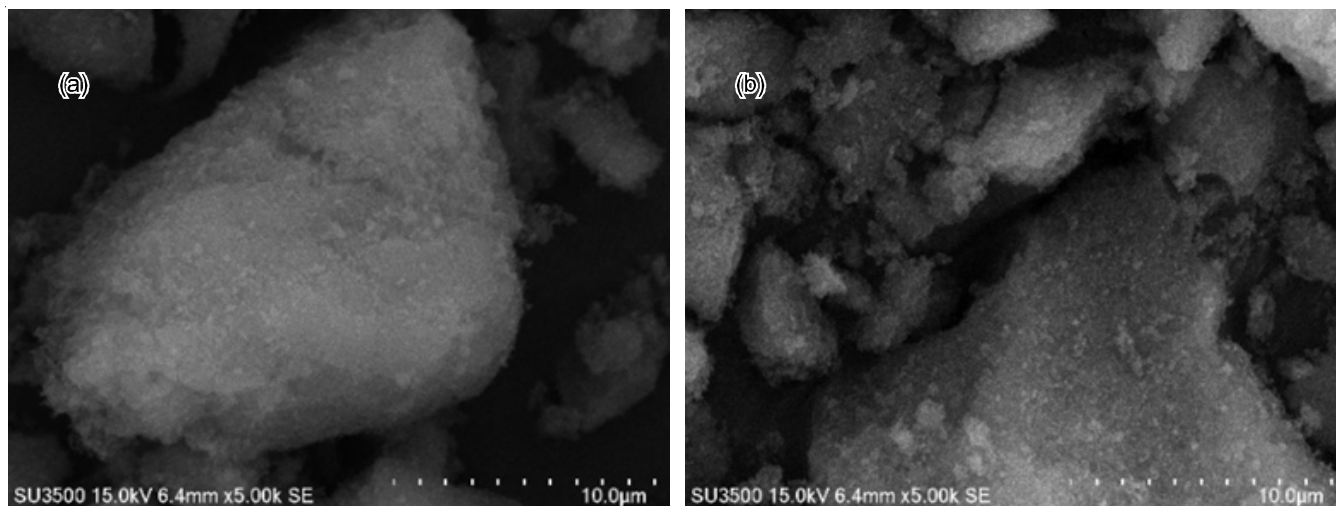


Fig. 2. SEM micrograph of $(\text{Cu-Ni})\text{O}_x@/\text{SiO}_2$ where (a) $\text{Cu:Ni} = 0.2:0.1$ and (b) $\text{Cu:Ni} = 0.15:0.15$

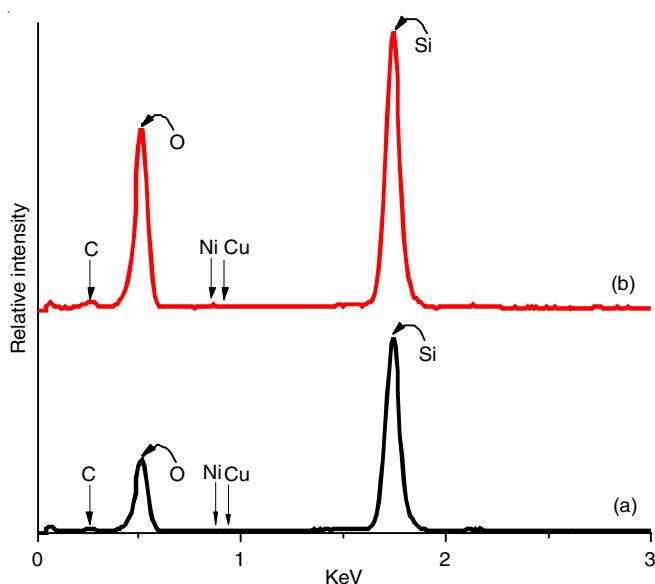


Fig. 3. EDX spectra of $(\text{Cu-Ni})\text{O}_x@/\text{SiO}_2$ where (a) $\text{Cu:Ni} = 0.2:0.1$ and (b) $\text{Cu:Ni} = 0.15:0.15$

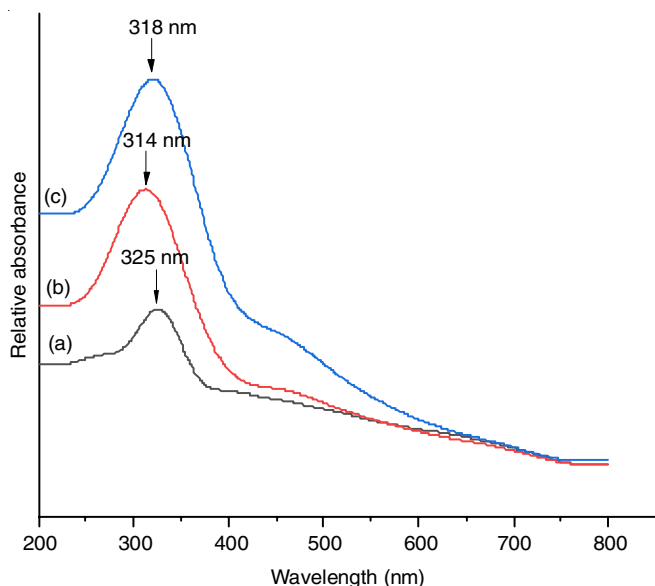


Fig. 4. UV-visible spectra $(\text{Cu-Ni})\text{O}_x@/\text{SiO}_2$ where $\text{Cu:Ni} =$ (a) 0.3:0, (b) 0.2:0.1 and (c) 0.15:0.15

The band gap energy affects the photocatalytic ability of a catalyst. Reflectance data are applied in the Kubelka-Munk equation [23] to calculate the band gap energy (E_g) of catalysts. The determination of band gap energy by the Kubelka-Munk method involves graphs of $h\nu$ vs. $(F(R'_{\infty} \times h\nu))^{1/2}$ presented in Fig. 5.

The band gap energy of $(\text{Cu-Ni})\text{O}_x@/\text{SiO}_2$ catalyst is described in Table-1. The CuO_x band gap energies (E_{g1} and E_{g2}) are as low as between 2.20 to 2.77 eV which are in agreement with the findings of Salavati-Niasari & Davar [24] and Dubal *et al.* [25]. Whereas the NiO_x has band gap energy in the range of 3.4-4.3 eV, as stated by Rifaya *et al.* [26] supporting nickel and copper oxides onto silica can cause lowering band gap energy of silica.

TABLE-1
BAND GAP ENERGY OF $(\text{Cu-Ni})\text{O}_x@/\text{SiO}_2$ CATALYST
WHERE $\text{Cu:Ni} =$ (a) 0.3:0, (b) 0.2:0.1 AND (c) 0.15:0.15

$(\text{Cu-Ni})\text{O}_x@/\text{SiO}_2$, Cu:Ni =	Band gap energy (eV)		
	E_{g1}	E_{g2}	E_{g3}
0.3:0	2.20	2.59	4.00
0.2:0.1	2.31	2.63	3.74
0.15:0.15	2.41	2.77	3.43

The methylene blue adsorption test on the catalyst is carried out in the dark environment, in order to avoid photocatalytic reactions. The concentration of methylene blue unadsorbed by the $(\text{Cu-Ni})\text{O}_x@/\text{SiO}_2$ catalyst where $\text{Cu:Ni} = 0.3:0$, 0.2:0.1 and 0.15:0.15 is observed at a period of time (Fig. 6). The addition of Ni in the catalysts decreases the adsorption of methylene blue.

Catalyst adsorption capacity was determined using the Langmuir and Freundlich equations [27], which then the isotherm patterns can be identified. Technically the Langmuir isotherm pattern is determined by using a graph relating between the concentration of methylene blue adsorbed on 1 g of catalyst (C/m) versus the unadsorbed methylene blue concentration (C). Whilst the Freundlich isotherm pattern is determined by a graph of relation between the log amount of methylene

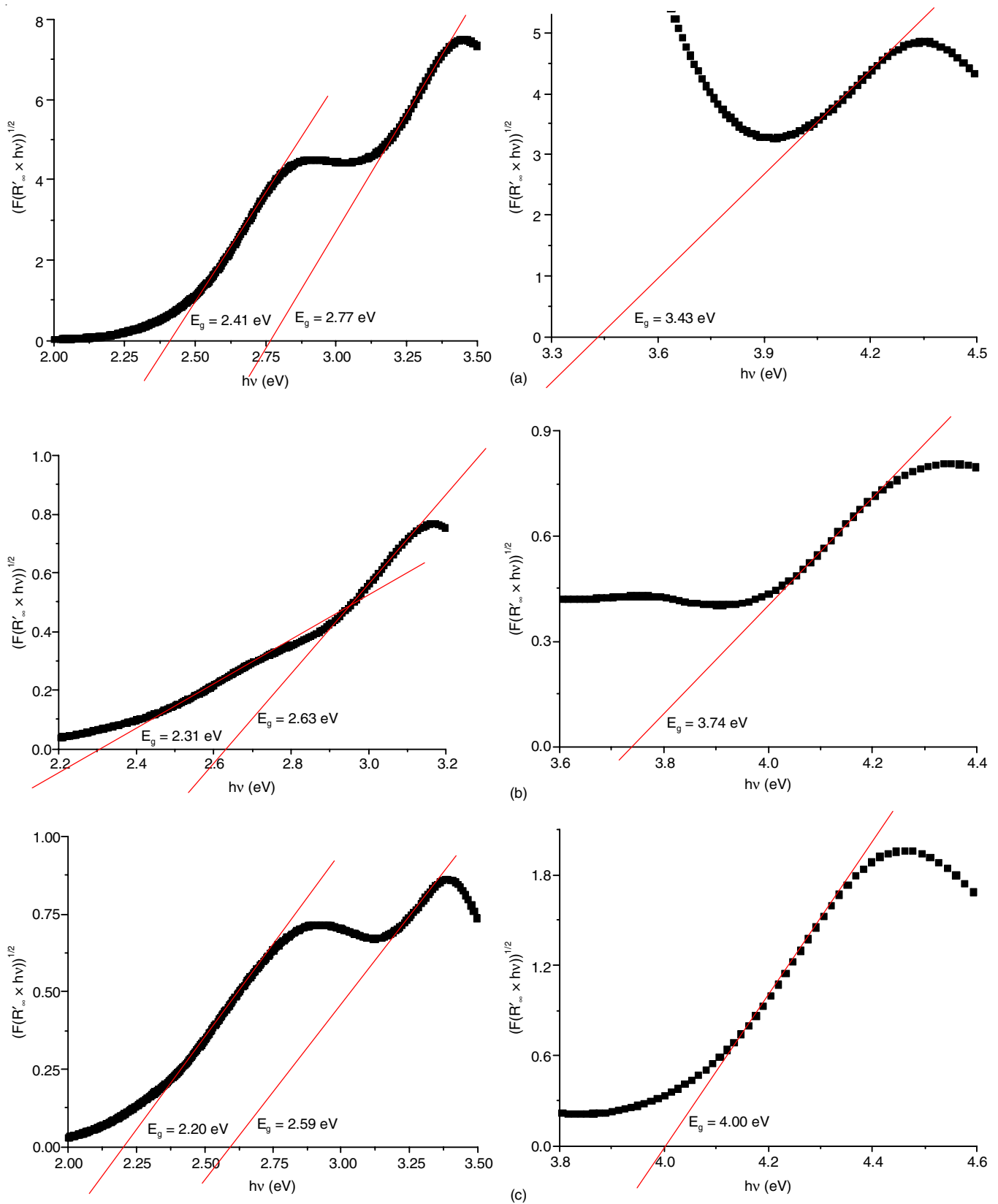


Fig. 5. Graphs of $h\nu$ vs. $(F(R'_{\infty} \times h\nu))^{1/2}$ to determine the band gap energy of $(\text{Cu-Ni})\text{O}_x@SiO_2$ catalyst where Cu:Ni = (a) 0.3:0, (b) 0.2:0.1 and (c) 0.15:0.15

blue adsorbed on every 1 g of catalyst ($\log X_m/m$) versus log concentration of unadsorbed methylene blue ($\log C$). Based on the graphs, line equations for catalyst can be formulated and listed in Table-2.

In general the R^2 of the Langmuir is more than the value of the Freundlich isotherm pattern. So it can be concluded that the adsorption of methylene blue by the $(\text{Cu-Ni})\text{O}_x@SiO_2$ catalysts follows the Langmuir isotherm pattern.

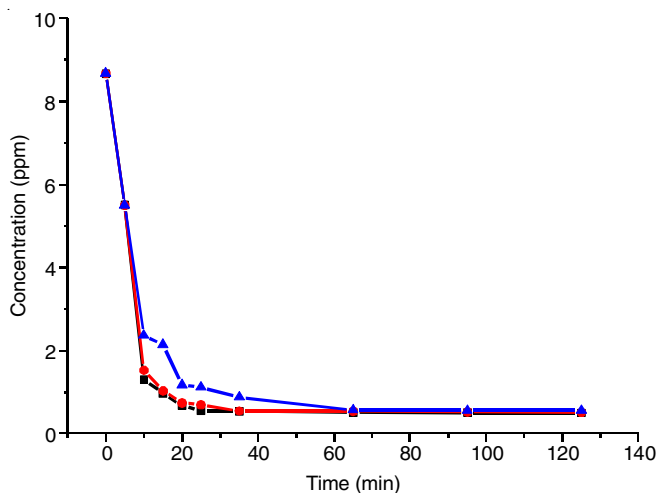


Fig. 6. Concentration of methylene blue unadsorbed by the $(\text{Cu-Ni})\text{O}_x/\text{SiO}_2$ catalyst where Cu:Ni = 0.3:0 (black line), 0.2:0.1 (red line) and 0.15:0.15 (blue line)

TABLE-2
LANGMUIR AND FREUNDLICH LINE
EQUATIONS OF $(\text{Cu-Ni})\text{O}_x/\text{SiO}_2$ CATALYST

$(\text{Cu-Ni})\text{O}_x/\text{SiO}_2$, Cu:Ni =	Langmuir line equations	Freundlich line equation
0.3:0	$y = 0.0698x - 0.0389$ $R^2 = 0.9953$	$y = -0.4585x + 1.5605$ $R^2 = 0.9551$
0.2:0.1	$y = 0.0707x - 0.0453$ $R^2 = 0.9922$	$y = -0.4662x + 1.579$ $R^2 = 0.926$
0.15:0.15	$y = 0.0665x - 0.0428$ $R^2 = 0.955$	$y = -0.369x + 1.5679$ $R^2 = 0.8247$

The adsorption capacity of the $(\text{Cu-Ni})\text{O}_x/\text{SiO}_2$ catalysts can be determined by a calculation using a line equation from the Langmuir isotherm pattern. The Langmuir equation model assumes that adsorption is occurred in the monolayer system of a homogeneous catalyst. The adsorption capacity of the $(\text{Cu-Ni})\text{O}_x/\text{SiO}_2$ catalysts is listed in Table-3. The $(\text{Cu-Ni})\text{O}_x/\text{SiO}_2$, Cu:Ni=0.30:0.00 has the highest adsorption capacity. This might be the oxide of copper blocks part of SiO_2 support surface, resulting a smaller surface area and so the smaller ability to adsorb methylene blue.

TABLE-3
ADSORPTION CAPACITY OF $(\text{Cu-Ni})\text{O}_x/\text{SiO}_2$ CATALYST

$(\text{Cu-Ni})\text{O}_x/\text{SiO}_2$, Cu:Ni =	Adsorption capacity (mol/g)
0.3:0.0	25.7069
0.2:0.1	22.0751
0.15:0.15	23.3645

The concentration of methylene blue decreases with increasing sunlight irradiation time. This proves that the photodegradation of methylene blue is occurred in the presence of the $(\text{Cu-Ni})\text{O}_x/\text{SiO}_2$ catalyst and sunlight. The effectiveness of degradation for the methylene blue in 120 min sunlight irradiation using the $(\text{Cu-Ni})\text{O}_x/\text{SiO}_2$, Cu:Ni = 0.3:0, 0.2:0.1 and 0.15:0.15 is 65.01 %, 63.48 % and 52.11 %, respectively.

Conclusion

The XRD and SEM-EDA methods not supported the presence of Cu and Ni specieses on the surface of silica. However

the band gap of the samples clearly indicate that the oxide of Cu and Ni is supported on the silica surface. In general crease the band gap of silica allowing the catalyst can be applied under visible light which is abundant in the sun light. The effectiveness of $(\text{Cu-Ni})\text{O}_x/\text{SiO}_2$, Cu:Ni = 0.3:0, 0.2:0.1 and 0.15:0.15 to degrade the methylene blue in 120 min sunlight irradiation is 65.01, 63.48 and 52.11 %, respectively.

CONFLICT OF INTEREST

The authors declare that there is no conflict of interests regarding the publication of this article.

REFERENCES

- S. Natarajan, H.C. Bajaj and R.J. Tayade, *J. Environ. Sci. (China)*, **65**, 201 (2018); <https://doi.org/10.1016/j.jes.2017.03.011>.
- N.M. Julkapli, S. Bagheri and S.B.A. Hamid, *Sci. World J.*, **2014**, Article ID 692307 (2014); <https://doi.org/10.1155/2014/692307>.
- B.A. Fil, C. Ozmetin and M. Korkmaz, *Bull. Korean Chem. Soc.*, **33**, 3184 (2012); <https://doi.org/10.5012/bkcs.2012.33.10.3184>.
- R.V. Kandisa, N. Saibaba KV, K.B. Shaik and R. Gopinath, *J. Bioremediat. Biodegrad.*, **7**, 371 (2016); <https://doi.org/10.4172/2155-6199.1000371>.
- M. Haddad, S. Abid, M. Hamdi and H. Bouallagui, *J. Environ. Manage.*, **223**, 936 (2018); <https://doi.org/10.1016/j.jenvman.2018.07.009>.
- L. Cai, T.B. Chen, S.W. Zheng, H.T. Liu and G.D. Zheng, *Chemosphere*, **201**, 127 (2018); <https://doi.org/10.1016/j.chemosphere.2018.02.177>.
- A.K. Verma, R.R. Dash and P. Bhunia, *J. Environ. Manage.*, **93**, 154 (2012); <https://doi.org/10.1016/j.jenvman.2011.09.012>.
- J. Mathieu-Denoncourt, C.J. Martyniuk, S.R. de Solla, V.K. Balakrishnan and V.S. Langlois, *Environ. Sci. Technol.*, **48**, 2952 (2014); <https://doi.org/10.1021/es500263x>.
- E. Grabowska, J. Reszczyńska and A. Zaleska, *Water Res.*, **46**, 5453 (2012); <https://doi.org/10.1016/j.watres.2012.07.048>.
- E. Forgacs, T. Cserhádi and G. Oros, *Environ. Int.*, **30**, 953 (2004); <https://doi.org/10.1016/j.envint.2004.02.001>.
- M.M. Khan, S.F. Adil and A. Al-Mayouf, *J. Saudi Chem. Soc.*, **19**, 462 (2015); <https://doi.org/10.1016/j.jscs.2015.04.003>.
- J. Zhou, F. Ren, S. Zhang, W. Wu, X. Xiao, Y. Liu and C. Jiang, *J. Mater. Chem. A Mater. Energy Sustain.*, **1**, 13128 (2013); <https://doi.org/10.1039/c3ta12540h>.
- D. Selishchev and D. Kozlov, *Molecules*, **19**, 21424 (2014); <https://doi.org/10.3390/molecules191221424>.
- O. Akhavan and E. Ghaderi, *Surf. Coat. Technol.*, **205**, 219 (2010); <https://doi.org/10.1016/j.surfcoat.2010.06.036>.
- Y.F. Chen, C.Y. Lee, M.Y. Yeng and H.T. Chiu, *J. Cryst. Growth*, **247**, 363 (2003); [https://doi.org/10.1016/S0022-0248\(02\)01938-3](https://doi.org/10.1016/S0022-0248(02)01938-3).
- S. Huang, L. Gu, N. Zhu, K. Feng, H. Yuan, Z. Lou, Y. Li and A. Shan, *Green Chem.*, **16**, 2696 (2014); <https://doi.org/10.1039/C3GC42496K>.
- X. Zhang and L. Zhang, *J. Phys. Chem. C*, **114**, 18198 (2010); <https://doi.org/10.1021/jp105118m>.
- L.S. Yoong, F.K. Chong and B.K. Dutta, *Energy*, **34**, 1652 (2009); <https://doi.org/10.1016/j.energy.2009.07.024>.
- R. Niishiro, H. Kato and A. Kudo, *Phys. Chem. Chem. Phys.*, **7**, 2241 (2005); <https://doi.org/10.1039/b502147b>.
- H. Nasution, E. Purnama, S. Kosela and J. Gunlazuardi, *Catal. Commun.*, **6**, 313 (2005); <https://doi.org/10.1016/j.catcom.2005.01.011>.

21. N. Srisittipokakun, Y. Ruangtaweep, W. Rachniyom, K. Boonin and J. Kaewkhao, *Results Phys.*, **7**, 3449 (2017); <https://doi.org/10.1016/j.rinp.2017.09.010>.
22. U. Holzwarth and N. Gibson, *Nat. Nanotechnol.*, **6**, 534 (2011); <https://doi.org/10.1038/nnano.2011.145>.
23. S. Akir, A. Barras, Y. Coffinier, M. Bououdina, R. Boukherroub and A.D. Omrani, *Ceram. Int.*, **42**, 10259 (2016); <https://doi.org/10.1016/j.ceramint.2016.03.153>.
24. M. Salavati-Niasari and F. Davar, *Mater. Lett.*, **63**, 441 (2009); <https://doi.org/10.1016/j.matlet.2008.11.023>.
25. D.P. Dubal, D.S. Dhawale, R.R. Salunkhe, V.S. Jamdade and C.D. Lokhande, *J. Alloys Compd.*, **492**, 26 (2010); <https://doi.org/10.1016/j.jallcom.2009.11.149>.
26. M.N. Rifaya, T. Theivasanthi and M. Alagar, *Nanosci. Nanotechnol.*, **2**, 134 (2012); <https://doi.org/10.5923/j.nn.20120205.01>.
27. A. Mittal, L. Kurup and J. Mittal, *J. Hazard. Mater.*, **146**, 243 (2007); <https://doi.org/10.1016/j.jhazmat.2006.12.012>.